NUCLEAR DATA AND MEASUREMENTS SERIES

ANL/NDM-13

Response of Several Threshold Reactions in Reference Fission Neutron Fields

by

Donald L. Smith and James W. Meadows

July 1975

ARGONNE NATIONAL LABORATORY,
ARGONNE, ILLINOIS 60439, U.S.A.

NUCLEAR DATA AND MEASUREMENTS SERIES

ANL/NDM-13

RESPONSE OF SEVERAL THRESHOLD REACTIONS IN REFERENCE FISSION NEUTRON FIELDS

by

Donald L. Smith and James W. Meadows

June 1975

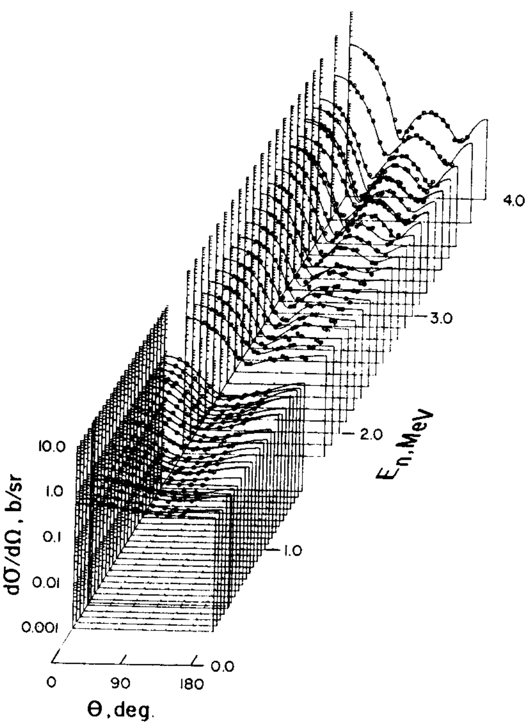

U of C - AUA - USAEC

ARGONNE NATIONAL LABORATORY,
ARGONNE, ILLINOIS 60439, U.S.A.

ANL/NDM-13

RESPONSE OF SEVERAL THRESHOLD REACTIONS IN REFERENCE FISSION NEUTRON FIELDS

by

Donald L. Smith and James W. Meadows

June 1975

In January 1975, the research and development functions of the former U.S. Atomic Energy Commission were incorporated into those of the U.S. Energy Research and Development Administration.

Applied Physics Division
Argonne National Laboratory
9700 South Cass Avenue
Argonne, Illinois 60439
U.S.A.

NUCLEAR DATA AND MEASUREMENTS SERIES

The Nuclear Data and Measurements Series presents results of studies in the field of microscopic nuclear data. The primary objective is the dissemination of information in the comprehensive form required for nuclear technology applications. This Series is devoted to: a) Measured microscopic nuclear parameters, b) Experimental techniques and facilities employed in data measurements, c) The analysis, correlation and interpretation of nuclear data, and d) The evaluation of nuclear data. Contributions to this Series are reviewed to assure technical competence and, unless otherwise stated, the contents can be formally referenced. This Series does not surplant formal journal publication but it does provide the more extensive information required for technological applications (e.g., tabulated numerical data) in a timely manner.

TABLE OF CONTENTS

	Page
ABSTRACT	3
1. INTRODUCTION	4
2. RENORMALIZATION OF (N,P) REACTION CROSS SECTION SETS TO COMPLY WITH ENDF/B-IV CROSS SECTIONS FOR MONITOR REACTIONS	6
3. COMPUTATION OF THE RESPONSE OF THRESHOLD REACTIONS IN REFERENCE FISSION NEUTRON FIELDS	8
4. DISCUSSION OF RESULTS	9
ACKNOWLEDGEMENT	12
APPENDIX A: PREPARATION AND CALIBRATION OF URANIUM DEPOSITS USED IN THRESHOLD REACTION MEASUREMENTS	13
APPENDIX B: ERRATA IN EARLIER REPORTS	15
REFERENCES	17
TABLES	18
FIGURES	33

RESPONSE OF SEVERAL THRESHOLD REACTIONS IN REFERENCE FISSION NEUTRON FIELDS*

by

Donald L. Smith and James W. Meadows

Argonne National Laboratory, Argonne, Illinois 60439, U.S.A.

ABSTRACT

Cross sections for (n,p) reactions on ^{27}Aℓ, ^{46,47,48}Ti, ^{54,56}Fe, ^{58}Ni, ^{59}Co, and ^{64}Zn and for ^{238}U fission have been measured in this laboratory relative to fission cross sections for ^{235}U or ^{238}U and the results of this work have been reported. These data have been renormalized to accommodate recent revisions of the ^{235}U and ^{238}U fission evaluated cross sections which are accouned for in the ENDF/B-IV files. The response of the renormalized data to two commonly used reference neutron fields have been investigated: i) pure thermal-neutron fission of ^{235}U, and ii) the spontaneous fission of ^{252}Cf. The results of this analysis and a comparison with corresponding recent information from the literature are discussed in this report. Two additional topics are addressed in appendices: i) the preparation and calibration of uranium deposits used in cross section measurements, and ii) errata in some earlier reports from our laboratory on this same general subject.

*This work performed under the auspices of the U.S. Energy Research and Development Administration.

1. INTRODUCTION

Data from monoenergetic measurements of cross section ratios for several (n,p) reactions relative to ^{235}U or ^{238}U fast-neutron fission and of the $^{238}U/^{235}U$ fast-neutron fission cross section ratio have been reported from this laboratory [1,2,3]. The results of the (n,p) measurements were expressed as final cross sections based on ENDF/B-III values for the appropriate fission cross sections [1,2,4], while the $^{238}U/^{235}U$ fission ratio data were reported as ratios [3]. In each instance, the data are very nearly representative of the monoenergetic quantities since various corrections were applied to compensate for the effects of finite geometry, multiple scattering, neutron energy spread and secondary neutron groups (see Ref. 1 for details).

Eye-guide curves were constructed for the (n,p) data which exhibit all significant features of the experimental values but eliminate redundancy and insignificant statistical fluctuations. A sufficient number of points were selected from these curves to enable reconstruction of the curves by interpolation, and these points are listed in Ref. 2 with the designation "evaluated cross sections". The use of the term "evaluated" is probably inappropriate since the curves were not generated from an unbiased consideration of all available data. The purpose of this exercise was to provide users of the data with an unambiguous representation of the monoenergetic cross sections which could then be used for a variety of applications (e.g., generation of multigroup cross section sets for reactor analysis).

Recently, the ENDF/B-IV files have become available [5] and these cross sections are utilized for most current applications, at least in the United States. Since our (n,p) reaction data were not explicitly presented in ratio form (although ratios could be computed from the information provided in Refs. 1 and 2), we decided that it would be worthwhile not only to make the ratios available but also to express the (n,p) cross sections in terms of the ENDF/B-IV fission cross sections. The renormalized cross sections would be comparable with other data sets in current use.

We chose to renormalize the eyeguide points for inclusion in this report. The experimental σ_{np}/σ_f ratios for the (n,p) reactions we have studied have been sent to the National Neutron Cross Section Center for inclusion in the CSISRS Experimental Data File [6]. While users of threshold reaction data for applications (e.g., in fast-neutron dosimetry) employ special forms for representation of the data (e.g., interval-averaged multigroup cross section sets), we chose not to alter the form of presentation of our results from that used in Ref. 2. The reason for this is that different applications call for different representations. By making use of point representations of the eyeguide curves and interpolation, one can generate data sets in any form desired.

Our (n,p) reaction data are intercalibrated since ratios to well-known fission cross sections were measured using a single set of uranium deposits and the same irradiation apparatus for all reactions. Furthermore, the counting facilities were calibrated using standards whose absolute source strengths were measured by coincidence techniques [1,2]. The (n,p)-to-fission cross section ratios depend upon characteristics of reaction product decay. The parameters which we have used are documented in Ref. 2. It was brought to our attention that a very useful test of our data would be to compute average cross sections for reference neutron fields [7]. The response of activation detectors to reference neutron fields is a standard method for evaluation and intercalibration of fast-neutron data for reactor dosimetry applications [7-10].

Two reference neutron fields commonly used for this purpose are: i) pure thermal fission of ^{235}U and, ii) spontaneous fission of ^{252}Cf. There are two important reasons for selection of these references. First, it is possible to produce quite good approximations to these fields experimentally. Secondly, the simple formula

$$X(E) = CE^{1/2} \exp(-1.5E/E_{av}) \tag{1}$$

provides a good representation of both these neutron spectra. Grundl and Eisenhauer [11], conducted a very careful evaluation of these fission-neutron spectra and concluded that Eq. (1) best represents the experimental data for ^{235}U thermal fission when E_{av} = 1.97 MeV. Likewise, the data for ^{252}Cf is well represented when E_{av} = 2.13 MeV is used. We have investigated the response of our (n,p) reaction data [1,] and the ^{238}U fission data of Meadows [3] to these standard neutron fields. The results of this analysis are presented in this report.

Two related items are discussed in appendices of this report. Appendix A is a detailed discussion of the procedure utilized in preparation of the uranium deposits used for all our measurements. We felt it worthwhile to present this information in this report since the calibration of monitor foils is a very important factor to be considered in the intercalibration of data measured in various laboratories. Appendix B contains errata from Refs. 1 and 2. These are mostly misprints. No errors have been found in our data acquisition and processing procedures which would affect the reported values.

2. RENORMALIZATION OF (N,P) REACTION CROSS SECTION SETS TO COMPLY WITH ENDF/B-IV CROSS SECTIONS FOR MONITOR REACTIONS

The cross sections to be renormalized appear in Tables XII thru XX of Ref. 2. The ENDF/B-III fission cross sections used previously appear in Table I of Ref. 2. The ENDF/B-IV fission cross sections to be used for renormalization appear in Table I of the present report. This table does not contain all the ENDF/B-IV values, but merely enough to accurately reproduce the shape of the curve over the energy region of interest for work. The renormalization procedure for the (n,p) cross sections is as follows:

If $\{(E_i, \sigma_{np,III,i})\}$ is a typical set of values from Ref. 2, then for energy E_i,

$$R_i = \sigma_{np,III,i}/\sigma_{f,III}(E_i) \tag{2}$$

where

R_i = cross section ratio for energy E_i,

$\sigma_{F,III}(E_i)$ = fission cross section for energy E_i, computed by linear interpolation of appropriate values from Table I, Ref. 2.

therefore,

$$\sigma_{np,IV,i} = R_i\sigma_{f,IV}(E_i) \tag{3}$$

yields the renormalized cross section, $\sigma_{np,IV,i}$, when

$\sigma_{f,IV}(E_i)$ = fission cross section for energy E_i, computed by linear interpolation of appropriate values from Table I of the present report.

Sets of values $\{(E_i, R_i, \sigma_{np,IV,i})\}$ resulting from the renormalization procedure appear in Table II thru X. ^{235}U fission cross sections were utilized for all data taken at energies below 4 MeV while ^{238}U fission cross sections were utilized for higher energy data. This is consistent with the measurement procedure [2].

It was not necessary to renormalize the ^{238}U fission ratio data of Meadows [3]. ^{238}U fission cross sections were computed from these ratios using ENDF/B-IV ^{235}U fission cross sections. An eyeguide was constructed for these cross section values and points were selected to represent the curve. These points are given in Table XI.

The points in Tables II thru XI represent the various (n,p) reaction cross sections and the ^{238}U fission cross section in such a fashion that the cross sections corresponding to arbitrary energies within the range of the data can be obtained by interpolation. Full logarithmic interpolation (see Section IV of Ref. 2 and Erratum No. 4 of Appendix B in the present report) is desirable since it provides a good representation of the cross sections in regions of high curvature (e.g., near threshold) and is nearly equivalent to linear interpolation in regions of gradual variation. However, linear interpolation was utilized for the renormalization procedure because this method was applied to the original experimental data to obtain the cross sections reported in Ref. 2. Computation of R_i values via Eq. (2) represents an "undoing" of part of the original data processing [1,2] in order to obtain unnormalized ratios. The fact that the original results were "smoothed" by eyeguides should not invalidate this procedure.

3. COMPUTATION OF THE RESPONSE OF THRESHOLD REACTIONS IN REFERENCE FISSION NEUTRON FIELDS

The response of the renormalized (n,p) cross sections and Meadows ^{238}U fission cross sections, based on ENDF/B-IV monitor cross sections, was investigated and the results are presented in this section.

For reaction process "j", let

$$\bar{\sigma}_j \; (E_{av}, E_{min}, E_{max}) \equiv \int_{E_{min}}^{E_{max}} dE \; X(E) \; \sigma_j(E) \; . \qquad (4)$$

where the monoenergetic cross section is $\sigma(E)$, and, if X(E) is given by Eq. 1, the constant C is chosen to yield the desired normalization

$$\int_0^\infty dE\ X(E) = 1\ . \qquad (5)$$

clearly,

$$\bar{\sigma}_j(E_{av}, E_{min}, E_{max}) < \bar{\sigma}_j(E_{av}, 0, \infty). \qquad (6)$$

let

$$\langle\sigma_j\rangle \equiv \bar{\sigma}_j(E_{av}, 0, \infty) = \text{spectrum averaged cross section.}$$

The quantity $\langle\sigma_j\rangle$ has been given the designation $\bar{\sigma}_f(X,j)$ by Grundl (e.g., Ref. 11) when X represents a fission neutron field. This notation appears to be widely accepted so we will comply with it in this report.

A point worthy of mention is summarized by Eq. (6). It is only meaningful to compare spectrum-averaged cross sections computed from monoenergetic data with the results of integral measurements where the monoenergetic data span essentially all of the response region of the reaction. A plot of the function X(E) $\sigma_j(E)$ provides a clear indication of whether this criterion is satisfied for a particular set of limits (E_{min}, E_{max}).

The results of our analysis appear in Figs. 1 thru 10 and are summarized in Table XII. It is clear from the figures that our data from near threshold to 10 MeV covers essentially all of the response range for the (n,p) reactions on ^{27}Aℓ, ^{47}Ti, ^{54}Fe, ^{58}Ni and ^{64}Zn, and for the fission of ^{238}U. The same cannot be said for the (n,p) reactions on ^{46,48}Ti, ^{56}Fe and ^{59}Co. These qualitative comments apply for both reference fission neutron fields.

4. DISCUSSION OF RESULTS

Values of $\bar{\sigma}(E_{av}, E_{min}, E_{max})$ from our work are compared with some representative results from the literature [5,9,10] in Table XIII. We indicate by (....) those values corresponding to incomplete integration of the response function. Otherwise, it is clear that our results for ^{235}U thermal fission are in quite good agreement with recent values from the literature. The values reported by Fabry [10] result from an evaluation of integral data. The values labelled ENDF/B-IV [5,13] were generated by integrating the evaluated cross sections in that file in a spectrum defined by Eq. (1) with E_{av} = 1.98 MeV (which is slightly different from the ^{235}U thermal fission spectrum of Grundl and Eisenhauer [11]). The evaluated values of Simons and McElroy are somewhat out of date now, but they have been included because the report which contains them is often referenced [9].

We have not assigned uncertainties to our averaged cross sections; however, in view of the quoted accuracies of the original data [1,2] it would seem that 10% is a reasonable upper limit. Considering the cross section uncertainties, our results appear to be entirely consistent with the evaluation by Fabry [11] and the ENDF/B-IV values [5,13]. A closer inspection of Table XIII and Figs. 1 thru 10 prompts us to offer the following subjective observations:

i) Generally, our results are in better agreement with the ENDF/B-IV integral values [10]. An exception is the $^{27}Al(n,p)^{27}Mg$ reaction. In view of the probable overlapping of error bars, the differences may not be significant.

ii) The shapes of the renormalized cross section curves in the vicinity of 5-7 MeV seem somewhat odd. This is particularly noticeable for reactions where the cross section is relatively flat at these energies (a good example is the $^{54}Fe(n,p)^{54}Mn$ reaction, Fig. 5). It is not hard to see why this occurs. These are noticeable differences in the ENDF/B-III and IV cross sections for ^{238}U fission for the region of

3-7 MeV. Furthermore, the ^{238}U fission cross section increases rapidly with energy between 5 and 7 MeV. We note that the shape peculiarity involves differences of $\sim$ 6% which are probably within the experimental uncertainties. Nevertheless, we feel that it is important to investigate the consequences of using ENDF/B-IV cross sections on the shapes of excitation functions since these effects are generally hidden when comparisons are based only upon integral data. Monoenergetic measurements are the only reliable method for investigation of excitation function structure. Regrettably, there is very little systematic work being done in this important area.

iii) The need for additional (n,p) reaction data for $^{46,48}Ti$, ^{56}Fe and ^{59}Co is apparent from our response curves. For various experimental reasons, these would be difficult measurements to make.

iv) There are no qualitative differences in the responses of the threshold reactions we have studied insofar as the two reference fission neutron fields are concerned. The ^{252}Cf spectrum is harder and consequently, the results of an absence of data above 10 MeV are more noticeable. An advantage of the ^{252}Cf source is that measurements can be made without reactors and the carefully designed irradiation cavities which are required to simulate the ^{235}U pure thermal fission field.

ACKNOWLEDGEMENT

We are indebted to Dr. J. A. Grundl for some valuable suggestions he provided during a recent meeting with one of the authors (DLS).

APPENDIX A

PREPARATION AND CALIBRATION OF URANIUM DEPOSITS USED IN THRESHOLD REACTION MEASUREMENTS

Most of the uranium deposits were prepared by vacuum evaporation of UF_4. Masking plates with 2.54-cm dia. holes were positioned in the vacuum chamber so that they were perpendicular to the line connecting the boat containing the UF_4 and the center of the hole. Distances ranged from 9 to 17 cm. Deposits were made on platinum, molybdenum or stainless steel. All plates had polished surfaces. They were thoroughly degreased and clamped tightly against the masks. Any deposits which appeared to have any problems with adherence of the evaporated material were discarded. Deposit thicknesses up to 1 mg/cm^2 were readily obtained in this way.

Since the evaporation method involved a large amount of waste, it was only used for materials which were in good supply. Deposits of other materials were prepared by electroplating. The uniformity of the electroplated deposits was not as good and adherence was poor for deposits thicker than $\sim$ 0.5 mg/cm^2.

^{235}U Deposits

The mass analysis of the material used in fabricating the ^{235}U-enriched deposits, given in Table XIV, is the result of three separate determinations: two conducted at Argonne National Laboratory, Illinois, and one at Argonne National Laboratory-West, Idaho. The errors are based on the scatter of the results or the quoted precision, whichever is larger. Ten 2.54-cm dia deposits on 0.13 mm thick platinum backings were prepared by vacuum evaporation. Deposit masses ranged from $\sim$ 0.48 to $\sim$ 2.5 mg. They were counted in both low-geometry and 2π alpha counters. The geometry factor of the low-geometry counter was 222.9 ± 0.7. Most of the error arose from the uncertainty in the thickness of the platinum and the difficulty of getting the soft material to lie flat against the support plate. A comparison of the low-geometry and 2π count rates indicated that a 2.6 ± 0.2% correction was required for back scattering from the platinum backing at zero deposit thickness. The deposits were dissolved from the backings and the amount of uranium determined by colorimetric comparison to standard solutions. The error, as determined from the difference of duplicate measurements, was ∿ 0.5%.

The specific activity computed from the above information was 2.065 ± 0.011 d/sec/μg. The calculated specific activity, based on recent half-life determinations [14-16], is 2.043 ± 0.015 d/sec/μg, a difference of 1.1%.

The ^{235}U-enriched deposits used for neutron monitoring were prepared by evaporating the above-mentioned material onto 0.25-mm thick, polished stainless steel plates. Ten 2.54-cm dia deposits were initially prepared with thicknesses ranging from ∿ 80 to ∿ 365 $\mu g/cm^2$. These deposits were counted in a low-geometry counter with a geometry factor of 221.7 ± 0.7 and also in a 2π counter. Comparison of the two count rates indicated a back scattering correction of 0.9%, in good agreement with the results for platinum, considering the difference in atomic number of the backing materials. The masses of each of the deposits are based on the low-geometry counts and the specific activity of the material used in fabrication.

^{238}U Deposits

The ^{238}U deposits were prepared from depleted uranium and since the activity was too low for counting in a low-geometry counter all counting was done in the 2π counter. Several 2.54-cm dia deposits were made by vacuum evaporation of UF_4 on 0.13-mm molybdenum plates. All were counted in a 2π counter and six were analyzed colorimetrically to determine the amount of uranium present. The mass of the material and the 2π-count rate are related by

$$W = R/(A + b\ R) \qquad \text{(A.1)}$$

where

W = mass of uranium

R = 2π-count rate

a = 0.5413 ± 0.0027

b = −0.0154 ± 0.0015

Other ^{238}U deposits were prepared from material containing only 6 ppm inpurities. Here, the activity was too low to make its accurate counting practical so the amount of uranium in the deposits was determined by a comparison of the fission rates with those of other calibrated deposits. Such comparisons were made with both ^{235}U-enriched and ^{238}U deposits using a technique described elsewhere [3].

Several of the deposits used in (n,p) cross section measurements were also used in measurement of the $^{238}U/^{235}U$ fission cross section ratio, and the results were in good agreement with fission cross section ratio measurements performed using deposits whose masses were determined by an independent method [3].

The calibrated uranium deposits used in threshold reaction cross section measurements in our laboratory are recounted at various intervals to insure that no uranium is physically lost with the passage of time.

APPENDIX B

ERRATA IN EARLIER REPORTS

The results of our work related to the measurement of (n,p) reaction cross sections have been made available in two reports issued from this laboratory [1,2]. Corrections for some errors found in these reports are presented in this appendix.

<u>Erratum No. 1</u>: Report ANL-7989 [1].

Eq. (C.4) in Appendix C should read:

$$\Theta_{Sk\ell} = \frac{\Theta^{max}_{S\ell}}{N_D} (k - \tfrac{1}{2}) \qquad \text{(C.4)}$$

<u>Erratum No. 2</u>: Report ANL-7989 [1].

Ref. 5 should read:

5. A. M. Bresesti, M. Bresesti, A. Rota, R. A. Rydin and L. Lesca, Nucl. Sci. Eng. <u>40</u>, 331 (1970).

Erratum No. 3: Report ANL-7989 [1].

Ref. 13 should read:

13. S. A. Cox and P. R. Hanley, "Performance of the ANL Dynamitron Tandem," IEE Trans. Nucl. Sci. 18, 108 (1971).

Erratum No. 4: Report ANL/NDM-10 [2].

Eqs. (2) and (3) should read:

$$a = (\ln E_2 \ln \sigma_1 - \ln E_1 \ln \sigma_2)/(\ln E_2 - \ln E_1) \tag{2}$$

$$b = (\ln \sigma_2 - \ln \sigma_1)/(\ln E_2 - \ln E_1) \tag{3}$$

Erratum No. 5: Report ANL/NDM-10 [2].

Ref. 11 should read:

11. S. A. Cox and P. R. Hanley, IEE Trans. Nucl. Sci. 18, 108 (1971).

REFERENCES

1. Donald L. Smith and James W. Meadows, Report ANL-7989, Argonne National Laboratory (1973).
2. Donald L. Smith and James W. Meadows, Report ANL/NDM-10, Argonne National Laboratory (1975).
3. J. W. Meadows, Nucl. Sci. Eng. 49, 310 (1972). Also, an additional paper has been accepted for publication in Nucl. Sci. Eng. and will be published in the near future.
4. Evaluated Neutron Data File, ENDF/B-III, National Neutron Cross Section Center, Brookhaven National Laboratory.
5. Evaluated Neutron Data File, ENDF/B-IV, National Neutron Cross Section Center, Brookhaven National Laboratory.
6. Experimental Data File, CSISRS, National Neutron Cross Section Center, Brookhaven National Laboratory.
7. J. A. Grundl, National Bureau of Standards, Washington, D. C. U.S.A. (Private communication).
8. A. M. Bresesti, M. Bresesti, A. Rota, R. A. Rydin and L. Lesca, Nucl. Sci. Eng. 40, 331 (1970).
9. R. L. Simons and W. N. McElroy, Report BNWL-1312, Battelle Northwest Laboratories (1970).
10. A. Fabry, Report BLG-465, Centre d'Etude de l'Energe Nucleaire (1972).
11. J. Grundl and C. Eisenhauer, Bull. Am. Phys. Soc. 20, 145 (1975).
12. B. E. Watt, Phys. Rev. 87, 1037 (1952).
13. B. A. Magurno and O. Ozer, Nucl. Tech. 25, 376 (1975).
14. P. de Bièvre, K. F. Lauer, H. Moret, G. Müschenborn, J. Spaepen, A. Spernol, R. Vaninbroukx and V. Verdingh from Chemical Nuclear Data Measurements and Methods, British Nuclear Energy Society, p 49-50, 20-22 September 1971.
15. A. H. Jaffey, K. F. Flynn, L. E. Glendenin, W. C. Bently and A. M. Essling, Phys. Rev. C4, 1889 (1971).
16. K. F. Flynn, A. H. Jaffey, W. C. Bentley and A. M. Essling, J. Inorg. Nucl. Chem. 34, 1121 (1972).

Table I

ENDF/B-IV Fission Cross Sections[a]

A. $^{235}U(n,f)$ Cross Sections

E_n (MeV)	σ_F (barn)	E_n (MeV)	σ_F (barn)	E_n (MeV)	σ_F (barn)
0.1	1.585	1.4	1.25	6.7	1.445
0.15	1.458	1.6	1.258	7.0	1.549
0.2	1.351	1.8	1.267	7.5	1.682
0.25	1.308	2.0	1.274	8.0	1.758
0.3	1.28	2.5	1.275	9.0	1.804
0.4	1.216	3.0	1.232	10.0	1.768
0.5	1.172	4.0	1.15	11.0	1.718
0.6	1.152	5.0	1.094	12.0	1.767
0.7	1.135	5.5	1.059	13.0	1.976
0.8	1.133	5.75	1.075	14.0	2.152
0.9	1.174	6.0	1.16	15.0	2.23
1.0	1.225	6.2	1.232		
1.2	1.258	6.5	1.358		

B. $^{238}U(n,f)$ Cross Sections

E_n (MeV)	σ_F (barn)	E_n (MeV)	σ_F (barn)	E_n (MeV)	σ_F (barn)	E_n (MeV)	σ_F (barn)
0.1	0.4×10^{-4}	0.92	0.01278	1.35	0.0933	2.5	0.555
0.3	0.7×10^{-4}	0.95	0.0163	1.4	0.1512	2.75	0.55
0.5	0.234×10^{-3}	0.97	0.01609	1.45	0.228	3.0	0.542
0.575	0.566×10^{-3}	1.0	0.01617	1.5	0.294	3.5	0.555
0.61	0.00124	1.05	0.01812	1.6	0.382	4.0	0.566
0.7	0.00134	1.1	0.0235	1.7	0.437	4.5	0.563
0.75	0.001985	1.15	0.0349	1.8	0.481	5.0	0.555
0.8	0.003116	1.2	0.0405	1.9	0.514	5.2	0.560
0.85	0.005871	1.25	0.0426	2.0	0.535	5.4	0.563
0.89	0.008716	1.3	0.0577	2.1	0.545	5.5	0.566

B. $^{238}U(n,f)$ Cross Sections

E_n (MeV)	σ_F (barn)	E_n (MeV)	σ_F (barn)	E_n (MeV)	σ_F (barn)	E_n (MeV)	σ_F (barn)
5.8	0.603	7.5	0.978	10.0	0.974	17.0	1.34
6.0	0.661	8.0	0.99	11.0	0.983	18.0	1.32
6.2	0.723	8.25	0.996	12.0	0.995	19.0	1.3
6.5	0.835	8.5	1.0	13.0	1.048	20.0	1.435
6.8	0.897	8.75	0.997	14.0	1.14		
7.0	0.93	9.0	0.992	15.0	1.26		
7.2	0.957	9.5	0.982	16.0	1.32		

[a]Ref. 5.

Table II

Cross Sections for the $^{27}Al(n,p)^{27}Mg$ Reaction Based on an Eyeguide to Experimental Data and ENDF/B-IV Fission Cross Sections

A. ^{235}U Monitor

E_n (MeV)	$(\sigma_{np}/\sigma_{F,235})$	σ_{np} (barn)	E_n (MeV)	$(\sigma_{np}/\sigma_{F,235})$	σ_{np} (barn)
.2800E 01	.3129E-03	.3909E-03	.3540E 01	.4693E-02	.5574E-02
.2950E 01	.6719E-03	.8007E-03	.3570E 01	.4703E-02	.5574E-02
.3000E 01	.8006E-03	.9663E-03	.3610E 01	.6026E-02	.7123E-02
.3050E 01	.9559E-03	.1174E-02	.3650E 01	.6046E-02	.7126E-02
.3120E 01	.1679E-02	.2052E-02	.3680E 01	.5710E-02	.6716E-02
.3200E 01	.1784E-02	.2169E-02	.3720E 01	.5729E-02	.6720E-02
.3240E 01	.2215E-02	.2685E-02	.3750E 01	.7776E-02	.9102E-02
.3270E 01	.2219E-02	.2685E-02	.3780E 01	.7795E-02	.9105E-02
.3300E 01	.1753E-02	.2117E-02	.3800E 01	.6477E-02	.7555E-02
.3340E 01	.1758E-02	.2117E-02	.3840E 01	.4006E-02	.4659E-02
.3400E 01	.3272E-02	.3924E-02	.3870E 01	.3927E-02	.4558E-02
.3460E 01	.6570E-02	.7846E-02	.3950E 01	.6201E-02	.7157E-02
.3500E 01	.6587E-02	.7845E-02			

B. ^{238}U Monitor

E_n (MeV)	$(\sigma_{np}/\sigma_{F,238})$	σ_{np} (barn)	E_n (MeV)	$(\sigma_{np}/\sigma_{F,238})$	σ_{np} (barn)
.4000E 01	.1330E-01	.7528E-02	.5280E 01	.4826E-01	.2708E-01
.4050E 01	.1237E-01	.6998E-02	.5330E 01	.4812E-01	.2704E-01
.4110E 01	.9557E-02	.5403E-02	.5370E 01	.5652E-01	.3180E-01
.4150E 01	.9557E-02	.5401E-02	.5420E 01	.5720E-01	.3224E-01
.4200E 01	.1312E-01	.7410E-02	.5450E 01	.5287E-01	.2985E-01
.4250E 01	.1686E-01	.9517E-02	.5470E 01	.5301E-01	.2996E-01
.4300E 01	.2154E-01	.1215E-01	.5500E 01	.6250E-01	.3537E-01
.4340E 01	.2154E-01	.1215E-01	.5525E 01	.7461E-01	.4246E-01
.4370E 01	.2023E-01	.1141E-01	.5575E 01	.7737E-01	.4451E-01
.4420E 01	.2023E-01	.1140E-01	.5625E 01	.8007E-01	.4655E-01
.4450E 01	.2248E-01	.1266E-01	.5675E 01	.9478E-01	.5569E-01
.4570E 01	.3654E-01	.2053E-01	.5710E 01	.1164E 00	.6890E-01
.4630E 01	.3693E-01	.2071E-01	.5740E 01	.1157E 00	.6891E-01
.4650E 01	.3318E-01	.1860E-01	.5800E 01	.7986E-01	.4816E-01
.4680E 01	.3281E-01	.1838E-01	.5875E 01	.7291E-01	.4555E-01
.4700E 01	.3469E-01	.1942E-01	.6000E 01	.6958E-01	.4599E-01
.4740E 01	.3469E-01	.1940E-01	.6250E 01	.6308E-01	.4678E-01
.4800E 01	.2532E-01	.1413E-01	.6500E 01	.5920E-01	.4943E-01
.4830E 01	.2533E-01	.1413E-01	.7000E 01	.5876E-01	.5465E-01
.4900E 01	.3566E-01	.1985E-01	.7500E 01	.6544E-01	.6400E-01
.4980E 01	.5257E-01	.2919E-01	.8000E 01	.7280E-01	.7207E-01
.5040E 01	.5258E-01	.2923E-01	.8500E 01	.7800E-01	.7800E-01
.5100E 01	.4934E-01	.2751E-01	.9000E 01	.8221E-01	.8155E-01
.5150E 01	.5424E-01	.3031E-01	.9500E 01	.8548E-01	.8394E-01
.5200E 01	.5595E-01	.3133E-01	.1000E 02	.8830E-01	.8600E-01
.5250E 01	.5207E-01	.2920E-01			

Table III

Cross Sections for the $^{46}Ti(n,p)^{46}Sc$ Reaction Based on an Eyeguide to Experimental Data and ENDF/B-IV Fission Cross Sections

A. ^{235}U Monitor

E_n (MeV)	$(\sigma_{np}/\sigma_{F,235})$	σ_{np} (barn)
.3600E 01	.1091E-01	.1290E-01
.3900E 01	.1700E-01	.1969E-01

B. ^{238}U Monitor

E_n (MeV)	$(\sigma_{np}/\sigma_{F,238})$	σ_{np} (barn)
.4000E 01	.4308E-01	.2438E-01
.4200E 01	.5996E-01	.3387E-01
.4300E 01	.6932E-01	.3911E-01
.4500E 01	.8430E-01	.4746E-01
.4700E 01	.1069E 00	.5984E-01
.5000E 01	.1352E 00	.7504E-01
.5200E 01	.1492E 00	.8355E-01
.5500E 01	.1679 00	.9503E-01
.6000E 01	.1909E 00	.1262E 00
.6500E 01	.1840E 00	.1536E 00
.7000E 01	.1784E 00	.1659E 00
.7500E 01	.1943E 00	.1900E 00
.8000E 01	.2093E 00	.2072E 00
.8500E 01	.2190E 00	.2190E 00
.9000E 01	.2280E 00	.2262E 00
.9500E 01	.2361E 00	.2319E 00
.1000E 02	.2402E 00	.2340E 00

Table IV

Cross Sections for the $^{47}Ti(n,p)^{47}Sc$
Reaction Based on an Eyeguide to Experimental
Data and ENDF/B-IV Fission Cross Sections

A. ^{235}U Monitor

E_n (MeV)	$(\sigma_{np}/\sigma_{F,235})$	σ_{np} (barn)
.9140E 00	.2078E-04	.2454E-04
.1130E 01	.9854E-03	.1228E-02
.1230E 01	.2338E-02	.2938E-02
.1300E 01	.2576E-02	.3230E-02
.1500E 01	.3128E-02	.3923E-02
.1600E 01	.3887E-02	.4890E-02
.1800E 01	.6756E-02	.8560E-02
.2000E 01	.1095E-01	.1395E-01
.2100E 01	.1333E-01	.1699E-01
.2200E 01	.1602E-01	.2042E-01
.2300E 01	.2292E-01	.2921E-01
.2330E 01	.2450E-01	.3123E-01
.2470E 01	.2475E-01	.3155E-01
.2600E 01	.2381E-01	.3015E-01
.2700E 01	.2414E-01	.3036E-01
.2900E 01	.2848E-01	.3533E-01
.3100E 01	.3517E-01	.4304E-01
.3300E 01	.4191E-01	.5060E-01
.3500E 01	.4854E-01	.5781E-01
.3800E 01	.5501E-01	.6416E-01

B. ^{238}U Monitor

E_n (MeV)	$(\sigma_{np}/\sigma_{F,238})$	σ_{np} (barn)
.4000E 01	.1236E 00	.6996E-01
.4300E 01	.1330E 00	.7504E-01
.4600E 01	.1387E 00	.7787E-01
.5000E 01	.1446E 00	.8025E-01
.5500E 01	.1554E 00	.8796E-01
.6000E 01	.1537E 00	.1016E 00
.6500E 01	.1287E 00	.1075E 00
.7000E 01	.1122E 00	.1043E 00
.8000E 01	.1203E 00	.1191E 00
.9000E 01	.1332E 00	.1321E 00
.1000E 02	.1448E 00	.1410E 00

Table V

Cross Sections for the $^{48}Ti(n,p)^{48}Sc$ Reaction Based on an Eyeguide to Experimental Data and ENDF/B-IV Fission Cross Sections for ^{238}U

E_n (MeV)	$(\sigma_{np}/\sigma_{F,238})$	σ_{np} (barn)
.4700E 01	.4312E-04	.2414E-04
.4900E 01	.1314E-03	.7314E-04
.5000E 01	.1634E-03	.9069E-04
.5100E 01	.1782E-03	.9935E-04
.5150E 01	.2001E-03	.1118E-03
.5200E 01	.3264E-03	.1828E-03
.5240E 01	.4652E-03	.2608E-03
.5300E 01	.5748E-03	.3228E-03
.5500E 01	.8571E-03	.4851E-03
.5600E 01	.9097E-03	.5261E-03
.5700E 01	.1132E-02	.6686E-03
.5900E 01	.2441E-02	.1543E-02
.6000E 01	.2913E-02	.1925E-02
.6200E 01	.3521E-02	.2546E-02
.6500E 01	.4762E-02	.3976E-02
.7000E 01	.6944E-02	.6458E-02
.7500E 01	.1022E-01	.9995E-02
.8000E 01	.1345E-01	.1332E-01
.8500E 01	.1640E-01	.1640E-01
.9000E 01	.2017E-01	.2001E-01
.9500E 01	.2391E-01	.2348E-01
.1000E 02	.2875E-01	.2800E-01

Table VI

Cross Sections for the $^{54}Fe(n,p)^{54}Mn$ Reaction Based on an Eyeguide to Experimental Data and ENDF/B-IV Fission Cross Sections

A. ^{235}U Monitor

E_n (MeV)	$(\sigma_{np}/\sigma_{F,235})$	σ_{np} (barn)
.2000E 01	.1065E-01	.1357E-01
.2200E 01	.1907E-01	.2430E-01
.2400E 01	.353 E-01	.4512E-01
.2600E 01	.5855E-01	.7415E-01
.2700E 01	.7518E-01	.9456E-01
.2800E 01	.9147E-01	.1143E 00
.3000E 01	.1089E 00	.1342E 00
.3200E 01	.1325E 00	.1611E 00
.3400E 01	.1722E 00	.2065E 00
.3500E 01	.1993E 00	.2374E 00
.3600E 01	.2112E 00	.2498E 00
.3700E 01	.2200E 00	.2584E 00
.3900E 01	.2353E 00	.2725E 00

B. ^{238}U Monitor

E_n (MeV)	$(\sigma_{np}/\sigma_{F,238})$	σ_{np} (barn)
.4100E 01	.5247E 00	.2967E 00
.4500E 01	.6257E 00	.3523E 00
.5000E 01	.7510E 00	.4168E 00
.5300E 01	.8010E 00	.4498E 00
.5600E 01	.7960E 00	.4604E 00
.6100E 01	.7202E 00	.4984E 00
.6500E 01	.6049E 00	.5051E 00
.7000E 01	.5021E 00	.4670E 00
.8500E 01	.4650E 00	.4650E 00
.1000E 02	.4723E 00	.4600E 00

Table VII

Cross Sections for the $^{56}Fe(n,p)^{56}Mn$ Reaction Based on an Eyeguide to Experimental Data and ENDF/B-IV Fission Cross Sections for ^{238}U

E_n (MeV)	$(\sigma_{np}/\sigma_{F,238})$	σ_{np} (barn)
.4000E 01	.1161E-04	.6571E-05
.4200E 01	.4216E-04	.2381E-04
.4300E 01	.8431E-04	.4757E-04
.4500E 01	.2585E-03	.1455E-03
.4700E 01	.6844E-03	.3831E-03
.4800E 01	.1069E-02	.5967E-03
.4900E 01	.1408E-02	.7837E-03
.5000E 01	.1784E-02	.9901E-03
.5200E 01	.3357E-02	.1880E-02
.5400E 01	.6108E-02	.3439E-02
.5500E 01	.8393E-02	.4750E-02
.5750E 01	.1443E-01	.8612E-02
.6000E 01	.1990E-01	.1315E-01
.6500E 01	.2574E-01	.2149E-01
.7000E 01	.2991E-01	.2782E-01
.7500E 01	.3579E-01	.3500E-01
.8500E 01	.4750E-01	.4750E-01
.9000E 01	.5407E-01	.5364E-01
.9500E 01	.5963E-01	.5856E-01
.1000E 02	.6417E-01	.6250E-01

Table VIII

Cross Sections for the $^{58}Ni(n,p)^{58}Co$ Reaction Based on an Eyeguide to Experimental Data and ENDF/B-IV Fission Cross Sections

A. ^{235}U Monitor

E_n (MeV)	$(\sigma_{np}/\sigma_{F,235})$	σ_{np} (barn)	E_n (MeV)	$(\sigma_{np}/\sigma_{F,235})$	σ_{np} (barn)
.5700E 00	.1729E-05	.2002E-05	.1500E 01	.1075E-01	.1348E-01
.6200E 00	.6078E-05	.6981E-05	.1600E 01	.1317E-01	.1657E-01
.6800E 00	.1746E-04	.1988E-04	.1700E 01	.1766E-01	.2230E-01
.7000E 00	.3149E-04	.3574E-04	.1800E 01	.2213E-01	.2804E-01
.7400E 00	.7900E-04	.8960E-04	.2000E 01	.3042E-01	.3876E-01
.8000E 00	.1677E-03	.1900E-03	.2200E 01	.4119E-01	.5249E-01
.8600E 00	.2593E-03	.3002E-03	.2400E 01	.6002E-01	.7651E-01
.9000E 00	.3632E-03	.4264E-03	.2500E 01	.7285E-01	.9288E-01
.1000E 01	.7287E-03	.8927E-03	.2650E 01	.9746E-01	.1230E 00
.1100E 01	.1616E-02	.2006E-02	.2850E 01	.1309E 00	.1630E 00
.1160E 01	.2825E-02	.3535E-02	.3000E 01	.1552E 00	.1912E 00
.1300E 01	.5313E-02	.6663E-02	.3250E 01	.1961E 00	.2376E 00
.1400E 01	.8758E-02	.1095E-01	.3500E 01	.2366E 00	.2818E 00
			.3750E 01	.2889E 00	.3382E 00

B. ^{238}U Monitor

E_n (MeV)	$(\sigma_{np}/\sigma_{F,238})$	σ_{np} (barn)
.4000E 01	.6631E 00	.3753E 00
.4250E 01	.7232E 00	.4082E 00
.4500E 01	.7680E 00	.4324E 00
.4750E 01	.7877E 00	.4403E 00
.5000E 01	.8261E 00	.4585E 00
.5500E 01	.9285E 00	.5255E 00
.5750E 01	.9304E 00	.5553E 00
.6000E 01	.9061E 00	.5989E 00
.7000E 01	.6090E 00	.5664E 00
.8000E 01	.5865E 00	.5806E 00
.9000E 01	.5750E 00	.5704E 00
.1000E 02	.5749E 00	.5600E 00

Table IX

Cross Sections for the $^{59}Co(n,p)^{59}Fe$ Reaction Based on an Eyeguide to Experimental Data and ENDF/B-IV Fission Cross Sections for ^{238}U

E_n (MeV)	$(\sigma_{np}/\sigma_{F,238})$	σ_{np} (barn)
.4300E 01	.1105E-01	.6234E-02
.5000E 01	.1765E-01	.9796E-02
.5500E 01	.2107E-01	.1193E-01
.6000E 01	.2314E-01	.1530E-01
.6500E 01	.2162E-01	.1805E-01
.7000E 01	.2062E-01	.1918E-01
.7500E 01	.2219E-01	.2170E-01
.8000E 01	.2447E-01	.2423E-01
.8500E 01	.2670E-01	.2670E-01
.9000E 01	.2935E-01	.2912E-01
.9500E 01	.3216E-01	.3158E-01
.1000E 02	.3501E-01	.3410E-01

Table X

Cross Sections for the $^{64}Zn(n,p)^{64}Cu$ Reaction Based on an Eyeguide to Experimental Data and ENDF/B-IV Fission Cross Sections

A. ^{235}U Monitor

E_n (MeV)	$(\sigma_{np}/\sigma_{F,235})$	σ_{np} (barn)
.1200E 01	.1734E-03	.2181E-03
.1400E 01	.4660E-03	.5825E-03
.1600E 01	.1150E-02	.1447E-02
.1800E 01	.2407E-02	.3050E-02
.2000E 01	.4867E-02	.6201E-02
.2300E 01	.1146E-01	.1461E-01
.2500E 01	.2015E-01	.2569E-01
.2700E 01	.3403E-01	.4280E-01
.2800E 01	.4333E-01	.5413E-01
.2900E 01	.5289E-01	.6562E-01
.3000E 01	.6190E-01	.7626E-01
.3250E 01	.8269E-01	.1002E 00
.3500E 01	.9534E-01	.1135E 00
.3750E 01	.1060E 00	.1241E 00

B. ^{238}U Monitor

E_n (MeV)	$(\sigma_{np}/\sigma_{F,238})$	σ_{np} (barn)
.4000E 01	.2379E 00	.1347E 00
.4500E 01	.2585E 00	.1495E 00
.5000E 01	.2835E 00	.1573E 00
.5250E 01	.2957E 00	.1658E 00
.5500E 01	.2893E 00	.1637E 00
.6000E 01	.2654E 00	.1754E 00
.7000E 01	.1795E 00	.1669E 00
.7500E 01	.1759E 00	.1720E 00
.8000E 01	.1810E 00	.1792E 00
.8500E 01	.1850E 00	.1850E 00
.9000E 01	.1896E 00	.1881E 00
.1000E 02	.1961E 00	.1910E 00

Table XI

Cross Sections for $^{238}U(n,f)$ Reaction
Based on an Eyeguide to Experimental Data and
ENDF/B-IV Fission Cross Sections for ^{235}U[a]

E_n (MeV)	$\sigma_{f,238}$ (barn)	E_n (MeV)	$\sigma_{f,238}$ (barn)
.8980E 00	.0122E 00	.2900E 01	.5400E 00
.1000E 01	.0158E 00	.3100E 01	.5330E 00
.1100E 01	.0273E 00	.3300E 01	.5360E 00
.1150E 01	.0352E 00	.3500E 01	.5480E 00
.1200E 01	.0440E 00	.3700E 01	.5530E 00
.1250E 01	.0425E 00	.4500E 01	.5600E 00
.1300E 01	.0615E 00	.5000E 01	.5550E 00
.1350E 01	.1000E 00	.5200E 01	.5560E 00
.1400E 01	.1800E 00	.5400E 01	.5620E 00
.1450E 01	.2600E 00	.5600E 01	.5770E 00
.1500E 01	.3450E 00	.6000E 01	.6610E 00
.1550E 01	.3850E 00	.6200E 01	.7340E 00
.1600E 01	.4050E 00	.6400E 01	.8240E 00
.1650E 01	.4250E 00	.6800E 01	.8860E 00
.1700E 01	.4500E 00	.7200E 01	.9650E 00
.1800E 01	.4750E 00	.7400E 01	.9920E 00
.1900E 01	.5150E 00	.7600E 01	.1010E 01
.2000E 01	.5280E 00	.8000E 01	.1031E 01
.2100E 01	.5280E 00	.8500E 01	.1048E 01
.2300E 01	.5420E 00	.9000E 01	.1068E 01
.2500E 01	.5490E 00	.9500E 01	.1073E 01
.2700E 01	.5480E 00	.1000E 02	.1048E 01

a $^{238}U/^{235}U$ fission ratio data from J.W. Meadows [3] were utilized in the preparation of this table.

Table XII

Summary of Response Calculation Results

Reaction "j"	E_{min} (MeV)	E_{max} (MeV)	$\bar{\sigma}_j(E_{av}, E_{min}, E_{max})$, mb[a]	
			E_{av} = 1.97 MeV	E_{av} = 2.13 MeV
$^{27}Al(n,p)^{27}Mg$	2.8	10.0	3.72	4.64
$^{46}Ti(n,p)^{46}Sc$	3.6	10.0	(10.0)	(12.6)
$^{47}Ti(n,p)^{47}Sc$	0.914	10.0	21.0	23.64
$^{48}Ti(n,p)^{48}Sc$	4.7	10.0	(0.227)	(0.315)
$^{54}Fe(n,p)^{54}Mn$	2.0	10.0	74.3	86.1
$^{56}Fe(n,p)^{56}Mn$	4.0	10.0	(0.913)	(1.23)
$^{58}Ni(n,p)^{58}Co$	0.57	10.0	99.4	114
$^{59}Co(n,p)^{59}Fe$	4.3	10.0	(1.11)	(1.42)
$^{64}Zn(n,p)^{64}Cu$	1.2	10.0	32.8	37.5
$^{238}U(n,f)$	0.898	10.0	293	314

[a] $\sigma_j(E_{av}, E_{min}, E_{max})$ computed using Eq. (4). E_{av} = 1.97 MeV corresponds to the neutron field for pure thermal fission of ^{235}U while E_{av} = 2.13 MeV corresponds to the spontaneous fission neutron field for ^{252}Cf [11]. Values expressed as (···) correspond to instances where our experimental data fail to cover a significant portion of the response range (see Figs. 1-10).

Table XIII

Comparison of Response Calculation Results for ^{235}U Thermal Fission Neutrons with Some Corresponding Values from the Literature

Reaction "j"	$\bar{\sigma}_j$, mb Present Work[a]	$\bar{\sigma}_f(X_{25,j})$, mb Simons and McElroy (1970)[b]	Fabry (1972)[c]	ENDF/B-IV (1975)[d]
$^{27}Al(n,p)^{27}Mg$ Good	3.72	-	4.0 ± 0.4	4.222
$^{46}Ti(n,p)^{46}Sc$ Lower En	(10.0)	11.3	12.3 ± 0.5	10.24
$^{47}Ti(n,p)^{47}Sc$ Sep. Iso. En ~10	21.0	17.2	20 ± 2	21.4
$^{48}Ti(n,p)^{48}Ti$	(0.227)	0.236	0.315 ± 0.02	0.194
$^{54}Fe(n,p)^{54}Mn$	74.3	76.3	82.5 ± 2	77.67
$^{56}Fe(n,p)^{56}Mn$	(0.913)	-	1.07 ± 0.06	1.145
$^{58}Ni(n,p)^{58}Co$	99.4	102.0	113 ± 2.5	101.5
$^{59}Co(n,p)^{59}Fe$	(1.11)	-	-	-
$^{64}Zn(n,p)^{64}Cu$	32.8	-	31 ± 1.5	-
$^{238}U(n,f)$	293	287.0	328 ± 10	295.4

[a] See Table XII.

[b] Ref. 9. Calculated using the Watt spectrum [12] and SAND-II Evaluated Reference Cross Section Library (1970 version).

[c] Ref. 10. Evaluated integral cross sections.

[d] Refs. 5 and 13.
Computed using Eq. (1) with E_{av} = 1.98 MeV and ENDF/B-IV monoenergetic (n,p) and ^{238}U fission cross sections.

Table XIV

Mass Analysis of ^{235}U Deposit Material

Isotope	% Abundance	Decay $t_{1/2}$ (Years)	Contribution to Specific Activity (d/sec/μg)
^{234}U	0.856	$(2.455 \pm 0.017) \times 10^5$ [a]	1.961 ± 0.014
^{235}U	93.249	$(7.0381 \pm 0.0048) \times 10^8$ [b]	0.074
^{236}U	0.332	$(2.3415 \pm 0.0014) \times 10^7$ [c]	0.008
^{238}U	5.526	$(4.4683 \pm 0.0034) \times 10^9$ [c]	5×10^{-6}

Total Specific Activity for ^{235}U Deposit Material:

Measured = 2.065 ± 0.011 d/sec/μg

Calculated = 2.043 ± 0.014 d/sec/μg

[a] Ref. 14.

[b] Ref. 15.

[c] Ref. 16.

FIGURE CAPTIONS

Figs. 1 thru 10. Response of the (n,p) reactions for ^{27}Al, $^{46,47,48}Ti$, $^{54,56}Fe$, ^{58}Ni, ^{59}Co and ^{64}Zn, and of fission of ^{238}U in reference neutron fields corresponding to i) thermal-neutron fission of ^{235}U and ii) spontaneous fission of ^{252}Cf. Symbols: (+) Points selected from eyeguide, $\sigma(E)$, to the experimental cross section data. Dashed line shows the reference neutron spectrum, $X(E)$. Solid line show the response function, $R(E) = X(E)\cdot\sigma(E)$. Plots are arbitrarily normalized to place maxima for each curve at the top border of frame.

....

ANL Negative Numbers

Fig. 1 (116-2749)

Fig. 2 (116-2745)

Fig. 3 (116-2746)

Fig. 4 (116-2753)

Fig. 5 (116-2750)

Fig. 6 (116-2752)

Fig. 7 (116-2751)

Fig. 8 (116-2748)

Fig. 9 (116-2747)

Fig. 10 (116-2754)

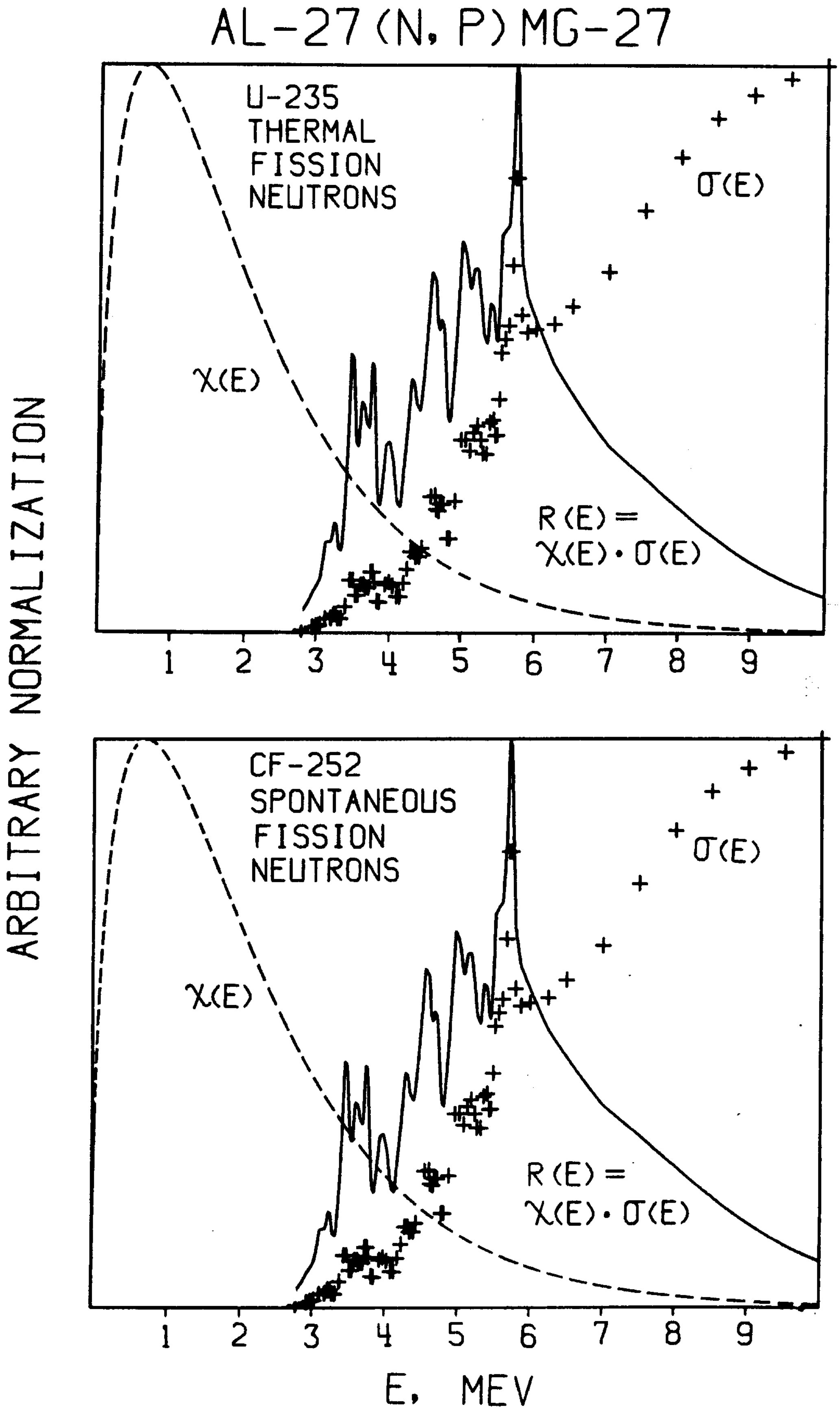
AL-27 (N, P) MG-27
U-235
THERMAL
FISSION
NEUTRONS
σ(E)
χ(E)
R(E) =
χ(E)·σ(E)
1 2 3 4 5 6 7 8 9
ARBITRARY NORMALIZATION
CF-252
SPONTANEOUS
FISSION
NEUTRONS
σ(E)
χ(E)
R(E) =
χ(E)·σ(E)
1 2 3 4 5 6 7 8 9
E, MEV

Fig. 2

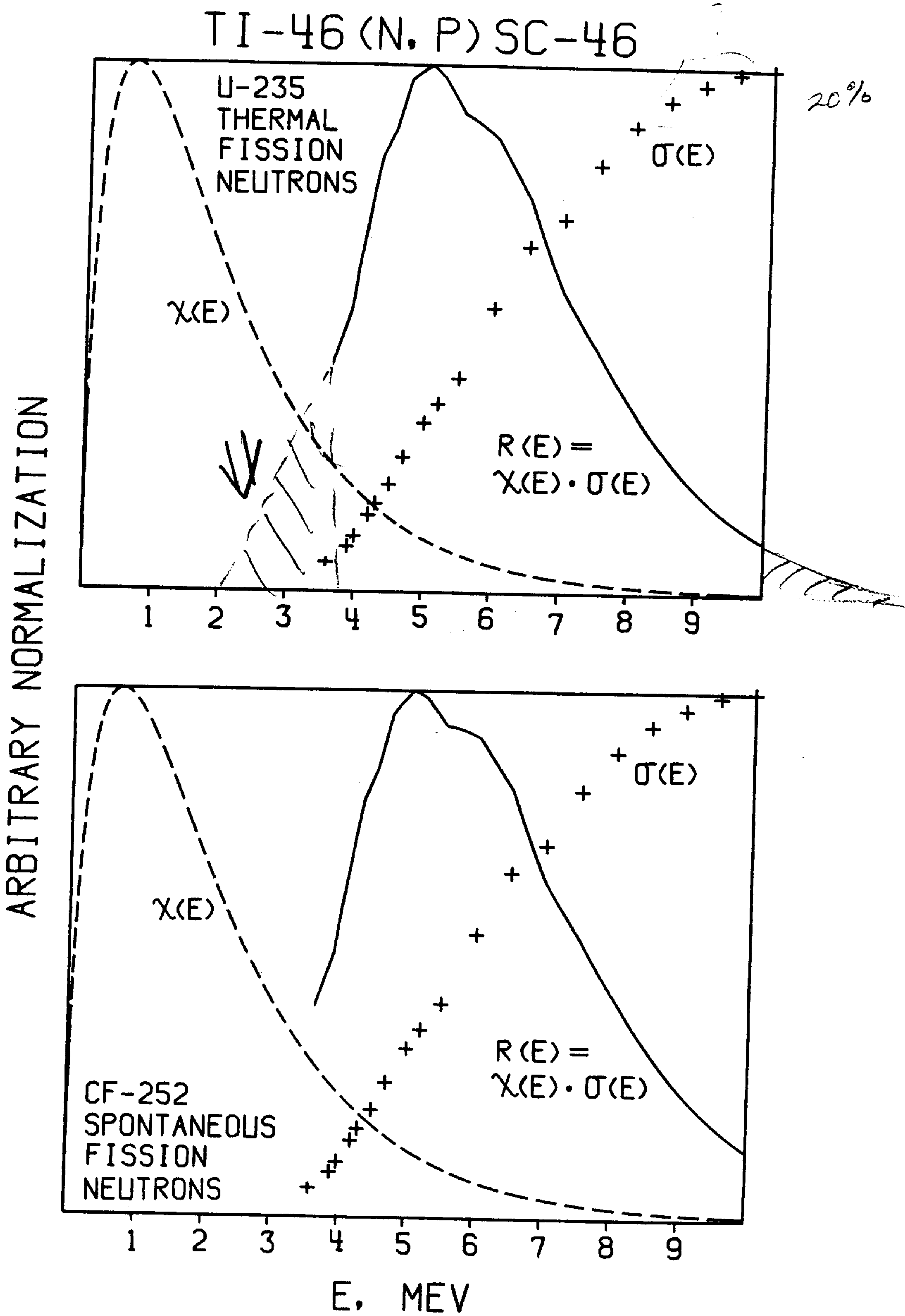
TI-46 (N, P) SC-46
20%
U-235
THERMAL
FISSION
NEUTRONS
σ(E)
χ(E)
R(E) =
χ(E) · σ(E)
1
2
3
4
5
6
7
8
9
σ(E)
χ(E)
R(E) =
χ(E) · σ(E)
CF-252
SPONTANEOUS
FISSION
NEUTRONS
1
2
3
4
5
6
7
8
9
ARBITRARY NORMALIZATION
E, MEV

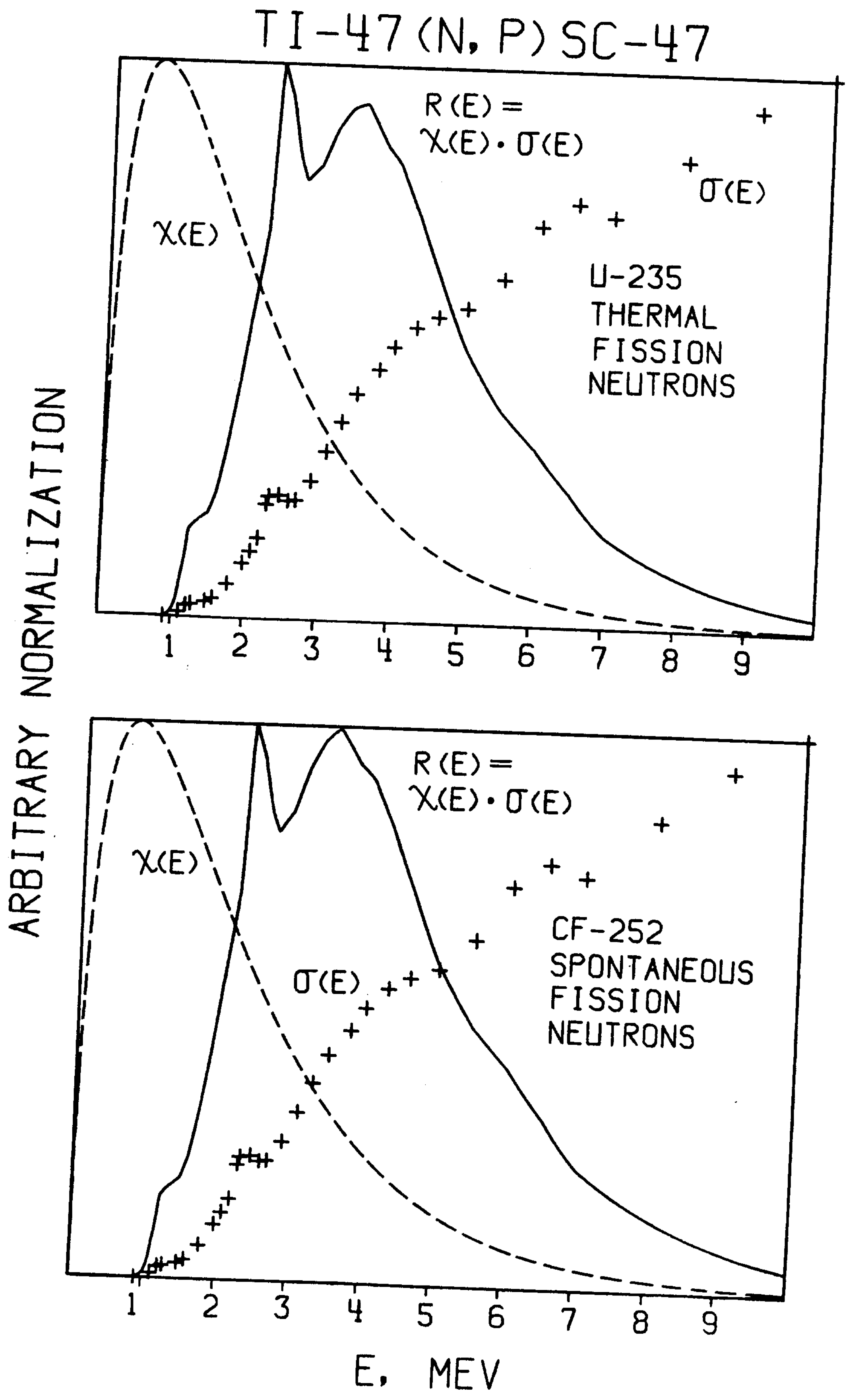
TI-47(N,P)SC-47
R(E) =
χ(E)·σ(E)
σ(E)
χ(E)
U-235
THERMAL
FISSION
NEUTRONS
1 2 3 4 5 6 7 8 9
ARBITRARY NORMALIZATION
R(E) =
χ(E)·σ(E)
χ(E)
σ(E)
CF-252
SPONTANEOUS
FISSION
NEUTRONS
1 2 3 4 5 6 7 8 9
E, MEV

Fig. 4

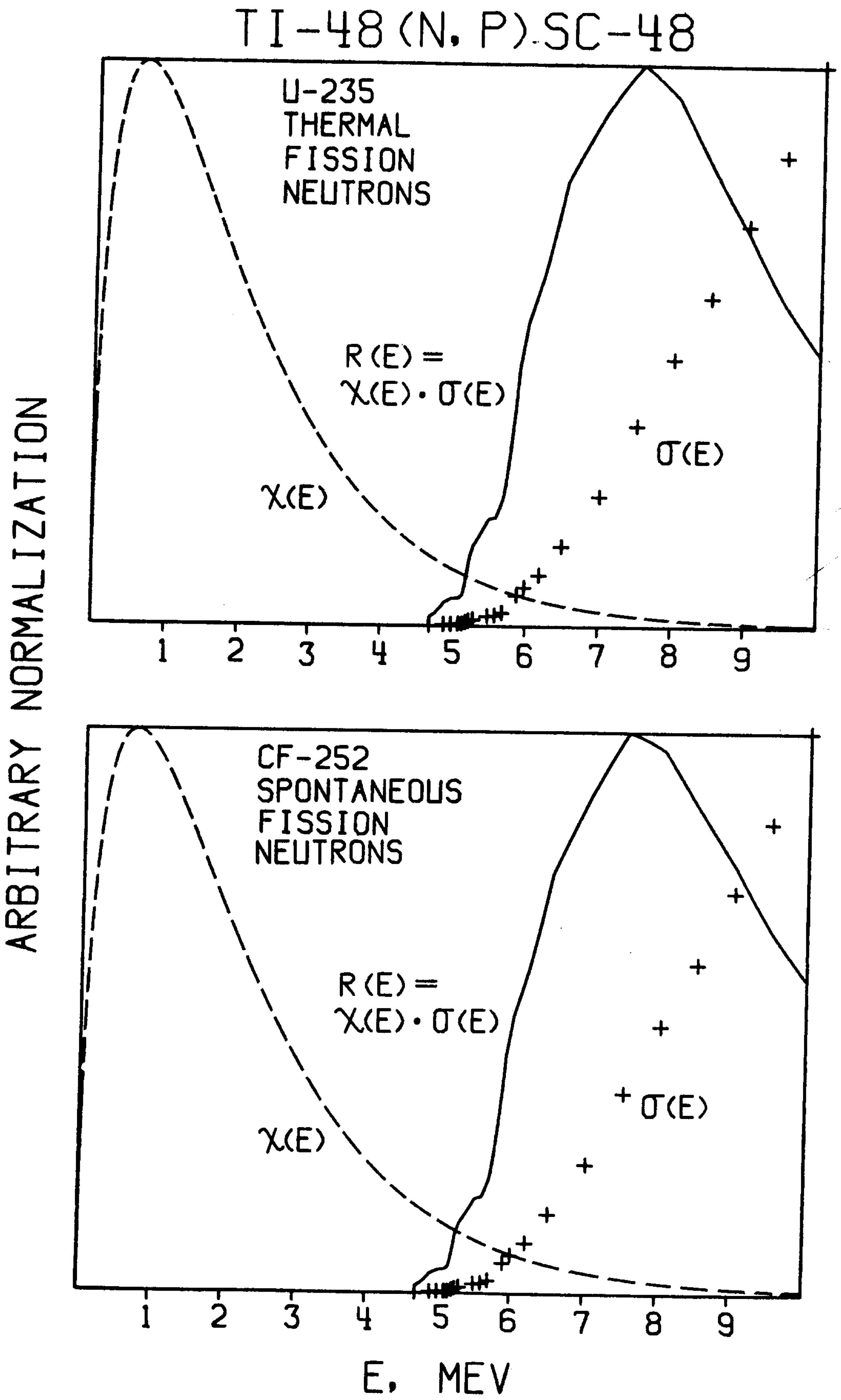

TI-48(N,P)SC-48
U-235
THERMAL
FISSION
NEUTRONS
R(E) =
χ(E)·σ(E)
σ(E)
χ(E)
1
2
3
4
5
6
7
8
9
CF-252
SPONTANEOUS
FISSION
NEUTRONS
R(E) =
χ(E)·σ(E)
σ(E)
χ(E)
1
2
3
4
5
6
7
8
9
ARBITRARY NORMALIZATION
E, MEV

30%

Fig. 5

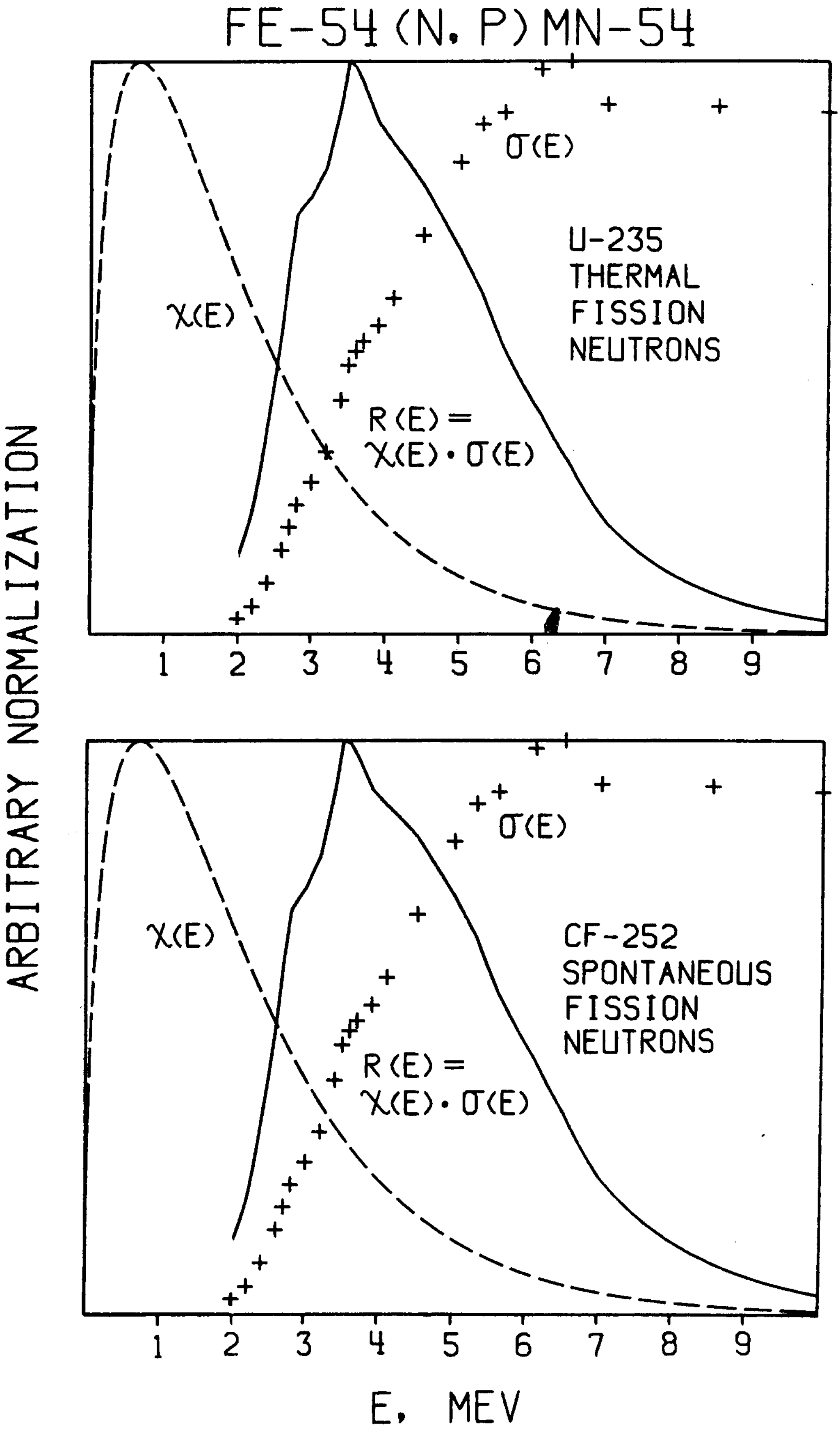
FE-54 (N, P) MN-54
ARBITRARY NORMALIZATION
σ(E)
χ(E)
U-235
THERMAL
FISSION
NEUTRONS
R(E) =
χ(E) · σ(E)
1
2
3
4
5
6
7
8
9
σ(E)
χ(E)
CF-252
SPONTANEOUS
FISSION
NEUTRONS
R(E) =
χ(E) · σ(E)
1
2
3
4
5
6
7
8
9
E, MEV

Fig. 6

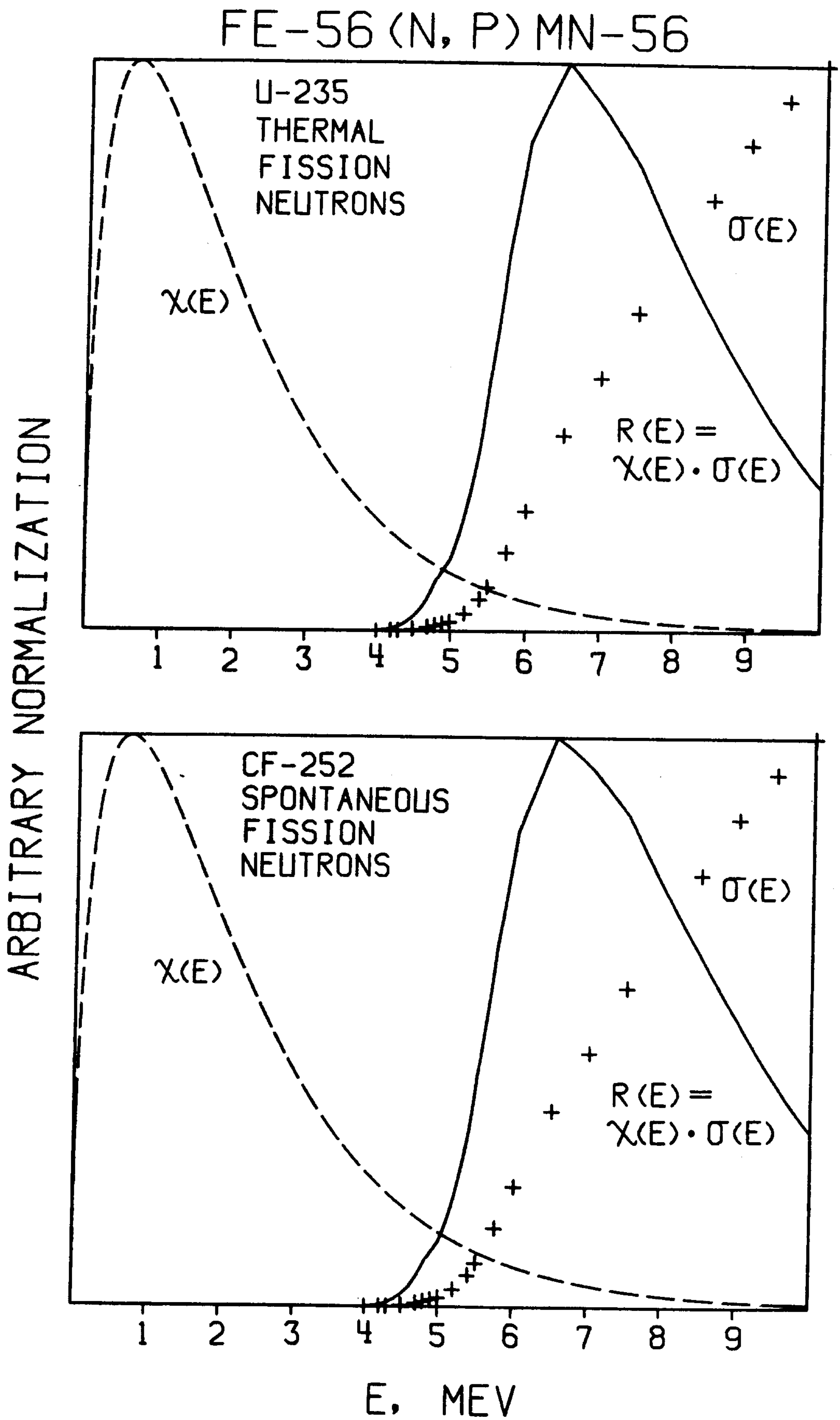
FE-56 (N, P) MN-56
U-235
THERMAL
FISSION
NEUTRONS
χ(E)
σ(E)
R(E) =
χ(E)·σ(E)
1 2 3 4 5 6 7 8 9
CF-252
SPONTANEOUS
FISSION
NEUTRONS
χ(E)
σ(E)
R(E) =
χ(E)·σ(E)
1 2 3 4 5 6 7 8 9
ARBITRARY NORMALIZATION
E, MEV

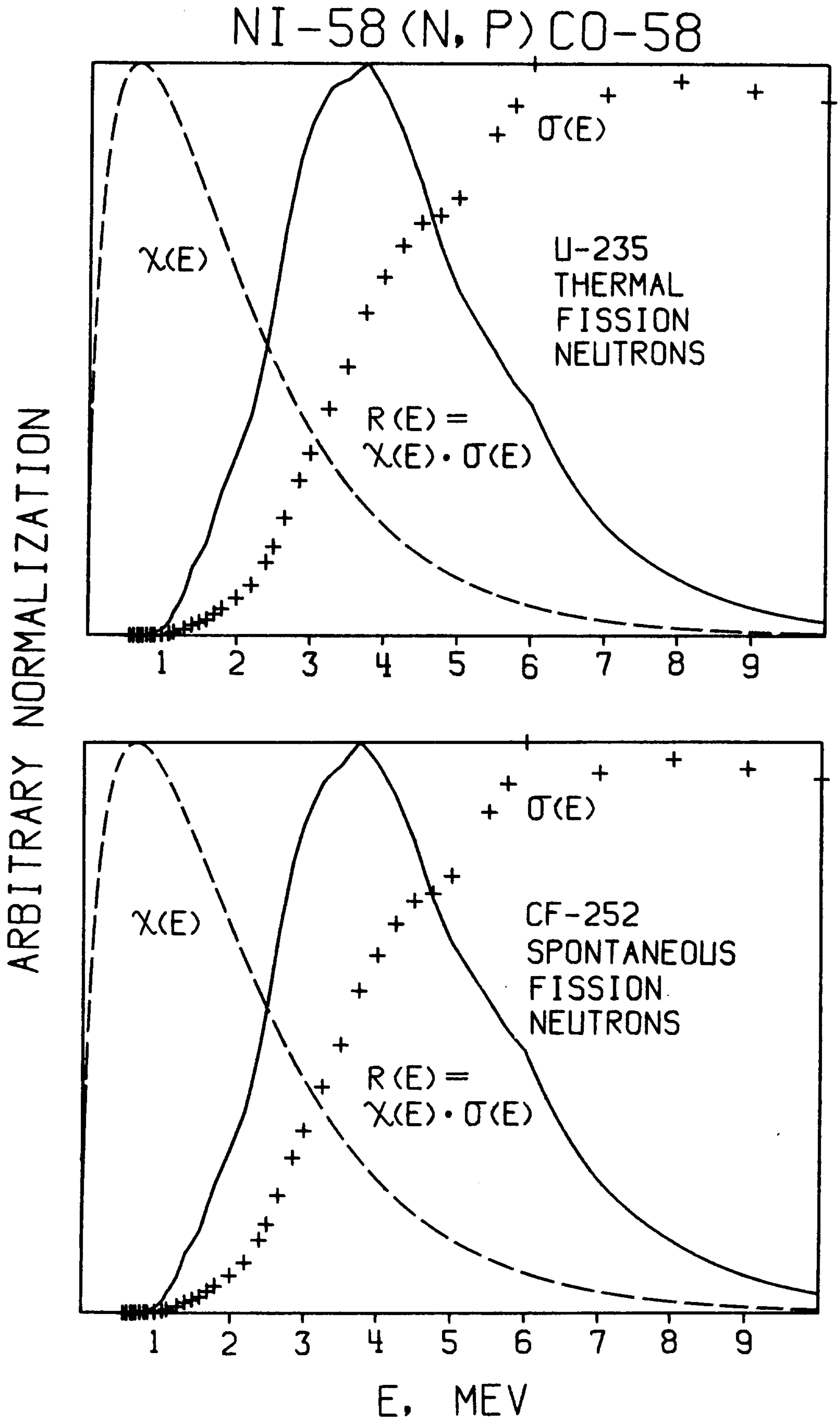
NI-58 (N, P) CO-58
ARBITRARY NORMALIZATION
σ(E)
χ(E)
U-235
THERMAL
FISSION
NEUTRONS
R(E) =
χ(E) · σ(E)
1
2
3
4
5
6
7
8
9
σ(E)
χ(E)
CF-252
SPONTANEOUS
FISSION
NEUTRONS
R(E) =
χ(E) · σ(E)
1
2
3
4
5
6
7
8
9
E, MEV

Fig. 8

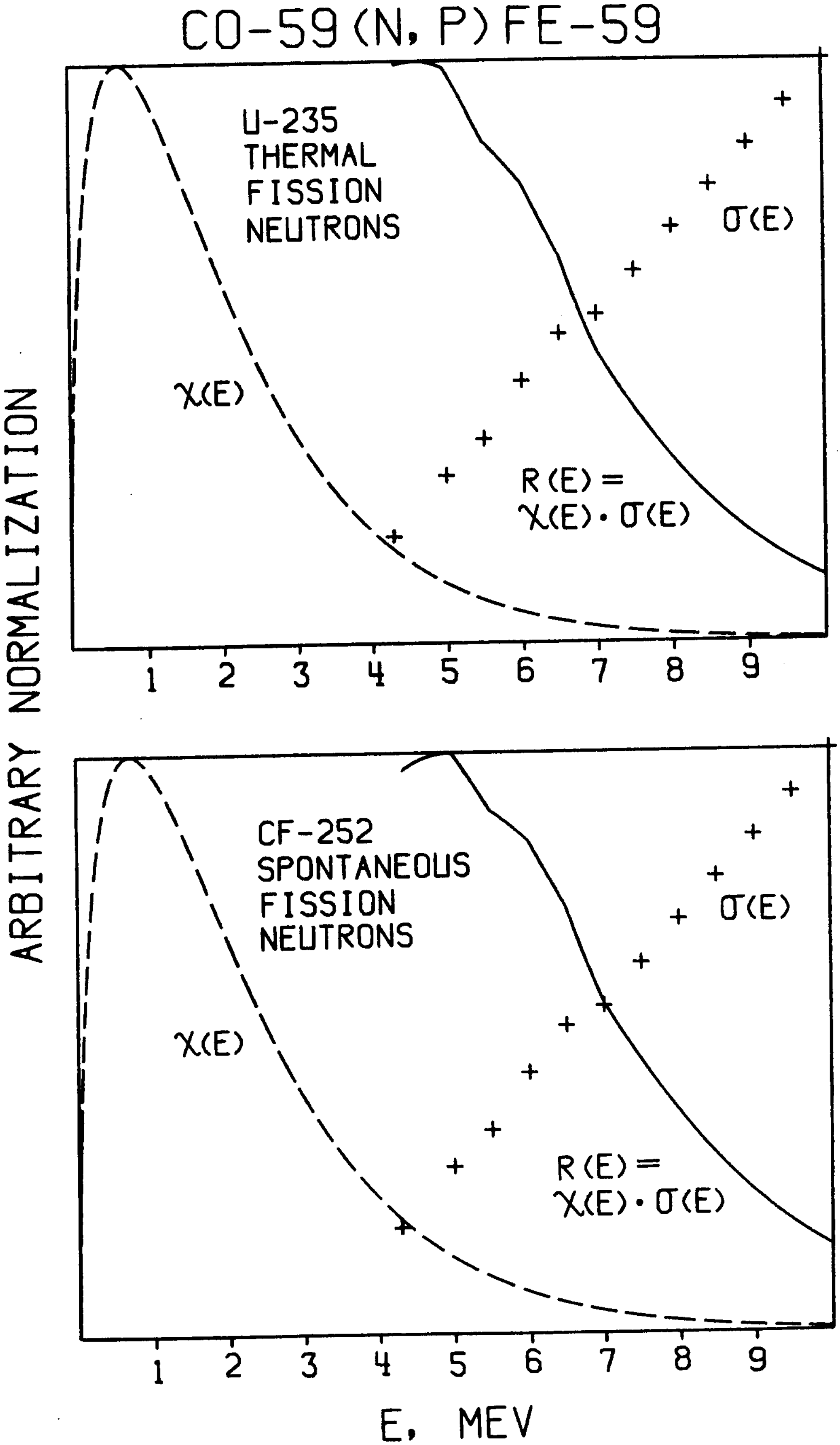
CO-59 (N, P) FE-59
ARBITRARY NORMALIZATION
U-235
THERMAL
FISSION
NEUTRONS
σ(E)
χ(E)
R(E) =
χ(E) · σ(E)
1 2 3 4 5 6 7 8 9
CF-252
SPONTANEOUS
FISSION
NEUTRONS
σ(E)
χ(E)
R(E) =
χ(E) · σ(E)
1 2 3 4 5 6 7 8 9
E, MEV

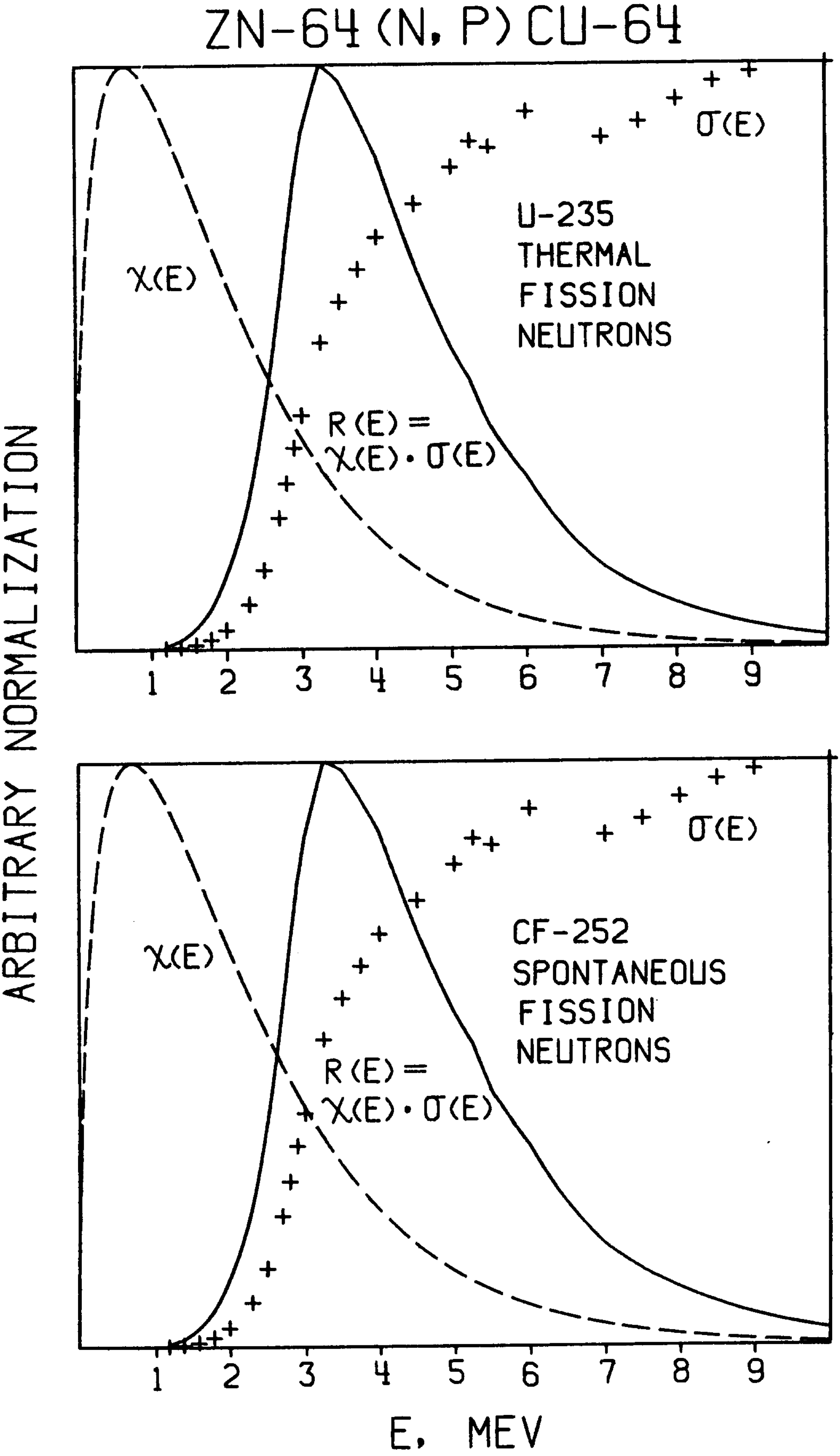
ZN-64 (N, P) CU-64
ARBITRARY NORMALIZATION
χ(E)
σ(E)
U-235
THERMAL
FISSION
NEUTRONS
R(E) =
χ(E) · σ(E)
1
2
3
4
5
6
7
8
9
χ(E)
σ(E)
CF-252
SPONTANEOUS
FISSION
NEUTRONS
R(E) =
χ(E) · σ(E)
1
2
3
4
5
6
7
8
9
E, MEV

Fig. 10

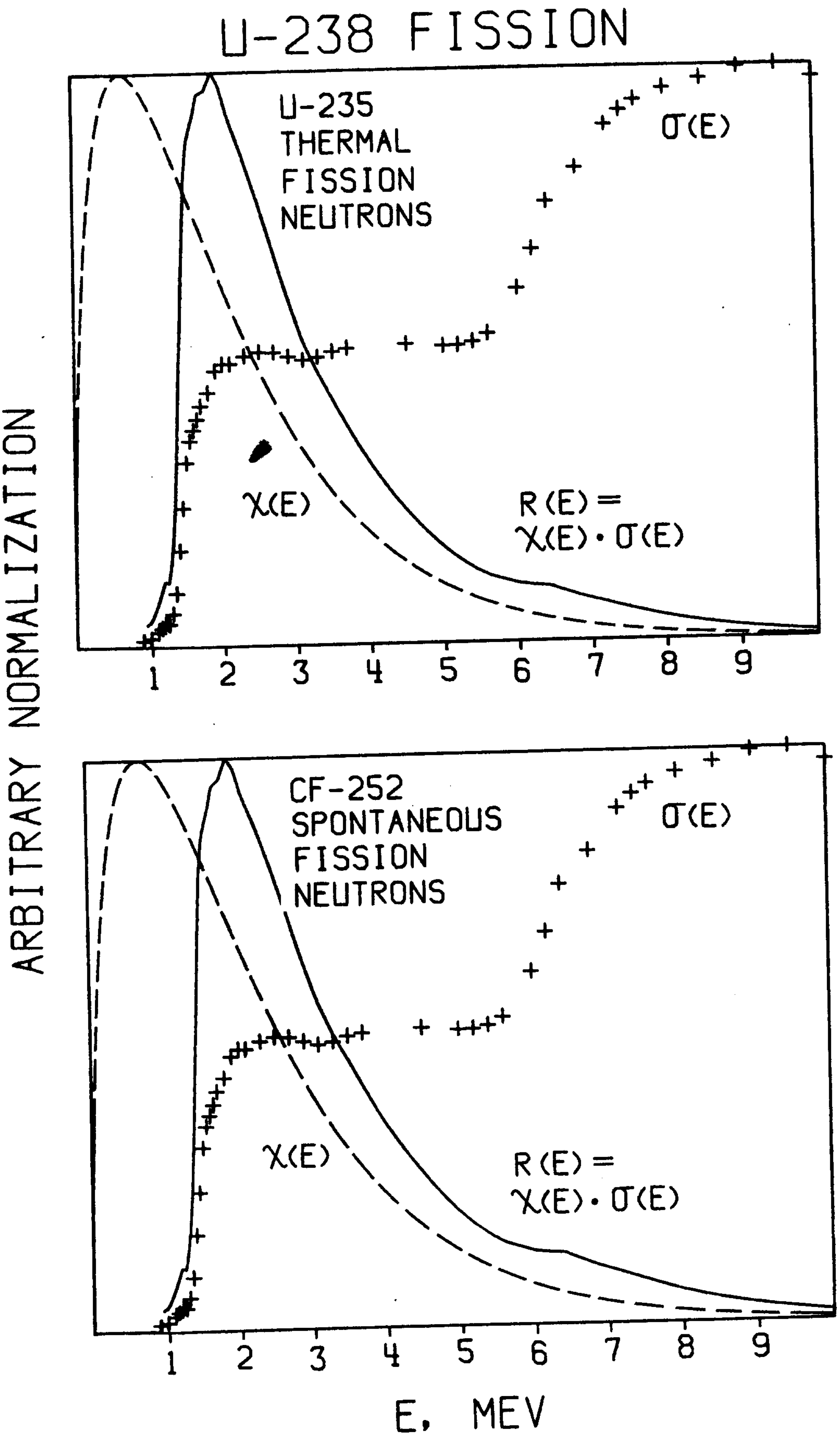
U-238 FISSION
U-235
THERMAL
FISSION
NEUTRONS
σ(E)
χ(E)
R(E) =
χ(E) · σ(E)
1 2 3 4 5 6 7 8 9
CF-252
SPONTANEOUS
FISSION
NEUTRONS
σ(E)
χ(E)
R(E) =
χ(E) · σ(E)
1 2 3 4 5 6 7 8 9
ARBITRARY NORMALIZATION
E, MEV